

Composites of Polymeric Gels and Magnetic Nanoparticles: Preparation and Drug Release Behavior

Nora J. François,¹ Sabina Allo,¹ Silvia E. Jacobo,² Marta E. Daraio¹

¹Laboratorio de Aplicaciones de Polímeros Hidrofílicos, Departamento de Química, Facultad de Ingeniería, Universidad de Buenos Aires, Paseo Colón 850, C1063ACV, Buenos Aires, Argentina

²Laboratorio de Físicoquímica de Materiales Cerámicos Electrónicos.; Departamento de Química, Facultad de Ingeniería, Universidad de Buenos Aires, Paseo Colón 850, C1063ACV, Buenos Aires, Argentina

Received 4 January 2007; accepted 8 February 2007

DOI 10.1002/app.26321

Published online 28 March 2007 in Wiley InterScience (www.interscience.wiley.com).

ABSTRACT: The article is concerned with the preparation of polymer–iron oxide nanocomposites and the study as drug-delivery matrices under the influence of applied magnetic field. Biocompatible materials were prepared by incorporating an aqueous ferrofluid in poly(vinyl alcohol) and scleroglucan (SCL) hydrogels, loaded with theophylline as model drug for release studies. The *in vitro* release profile was obtained using a flat Franz cell and the kinetic parameters were derived applying a semiempirical power law. A magnetic characterization of nanoparticles contained in the ferrofluid was performed by obtaining the magnetization curve. For both systems, the observed drug release profiles decreased when a uniform external mag-

netic field is applied suggesting they can be used as environmental responsive matrices for biomedical applications. Dynamic rheological measurements show that a higher storage modulus and a more compact structure are obtained by incorporating the ferrofluid into the hydrogels. These rheological results and environmental electron scanning microscopy micrographs point to an understanding of release behavior once the magnetic field is applied. © 2007 Wiley Periodicals, Inc. *J Appl Polym Sci* 105: 647–655, 2007

Key words: scleroglucan; polyvinyl alcohol; composites; stimuli-sensitive polymers; drug-delivery systems

INTRODUCTION

In the recent years, nanotechnology has developed to such a degree that it has been possible to produce, characterize, and make use of the functional properties of nanoparticles for biomedical applications.^{1,2} The use of small iron oxide particles in diagnostics has been experienced for nearly 40 years.³ Increased investigations with several types of iron oxides have been carried out in the field of nanosized magnetic particles (mostly maghemite γ -Fe₂O₃, or magnetite, Fe₃O₄, single domains of about 5–20 nm in diameter), among which magnetite is a very promising candidate since its biocompatibility has been verified.⁴ They are used for *in vivo* treatments, such as contrast agent for magnetic resonance imaging. The coating of these particles by organic or inorganic materials provides functional groups at the surface with the possibility to be functionalized with drugs. The application of an external magnetic field allows delivering these particles (beads) to a selected region

leading to drug targeting.⁵ Also, magnetic poly(ethyl-2-cyanoacrylate) nanoparticles were proposed as a highly versatile magnetic drug carrier with sustained release behavior.⁶

However, to our knowledge, there are scarce references in the field of magnetic sensitive gels specifically designed for matrix drug-delivery systems.

Environmental responsive polymeric gels belong to the class of materials capable of changing its physical properties in response to external stimuli. Because of this behavior, these versatile materials are expected to have a wide application in extended fields.⁷ In particular, magnetic field sensitive gels, called ferrogels, represent a new type of composites, consisting of small magnetic particles, usually in the nanometer range, dispersed in an elastic polymeric matrix.⁸ In a recent work, ferrogels of micron-sized magnetite particles and polyvinylalcohol (PVA) were evaluated for artificial muscle or soft actuator applications.⁹ Biodegradable gels with magneto-elastic properties have been synthesized using hydroxypropylcellulose and maghemite.¹⁰ The incorporated colloidal particles connect the shape and physical properties of the gel to the external field, owing to interactions between solid particles and polymer chains.^{11,12} Zrínyi et al. reported that ferrogels can undergo controllable changes in shape by the influence of an external magnetic field.¹³ Recently, Liu

Correspondence to: M. E. Daraio (medit@fi.uba.ar).

Contract grant sponsor: University of Buenos Aires; contract grant numbers: UBACyT I032, UBACyT I055.

et al. have reported the preparation of a ferrogel by mixing PVA hydrogels and Fe_3O_4 magnetic particles using freezing-thawing cycles. For these novel materials, rapid to slow drug release is achievable when the magnetic field is switched from "off" to "on" mode,¹⁴ which affects the deformation of the gel.

Environmentally sensitive hydrogels for drug delivery require polymeric networks with biocompatibility and biodegradability as essential requirements for successful applications. Taking into account these characteristics, in this work, composites based on PVA and scleroglucan (SCL) were assayed.

PVA is a synthetic biocompatible polymer that has been studied intensively because of its good gel and film forming characteristics. These properties allow its broad use in pharmaceutical and biomedical applications.¹⁵ Glutaraldehyde (GTA) is an efficient crosslinking agent commonly used to form PVA gels that has received widespread acceptance. The toxicity of GTA-crosslinked materials is often due to the presence of nonreacted aldehyde, which can cause local inflammation and calcification.¹⁶ However, it has been reported that when the concentration of GTA used to prepare gelatin membranes was lower than 0.1% w/w, the cell viability assay indicated the biocompatible nature of membranes.¹⁷ Magnetic films obtained from gels with a GTA-crosslinked PVA network have been described biocompatible, stable, and possessing the magnetic properties of the nanoparticles.¹⁸ In a recent work, the preparation of PVA magnetic films from an aqueous ferrofluid has been reported.¹⁹

SCL is a hydrogel-forming neutral polysaccharide, produced by fungi, having features such as high biocompatibility, biodegradability, bioadhesivity, chemical, and thermal resistance making it particularly well suited for drug-delivery applications. In aqueous solution, this polysaccharide adopts a stable triple-stranded helical conformation held together by hydrogen bonds.²⁰ In previous works, we studied SCL hydrogels as matrices for controlled release.²¹⁻²³

Two systems have been prepared and studied as follows:

- i. a film of PVA, chemically crosslinked with GTA, added with an aqueous magnetic colloidal suspension (a stabilized magnetite sol) and
- ii. a physically crosslinked hydrogel, obtained with SCL that swells in water in the presence of a magnetite sol giving a novel composite system.

To gain an understanding about these composites as potential drug-delivery systems, they were prepared in the presence of a model drug for release studies, theophylline (Th), previously dissolved in the aqueous phase.

Both systems were subjected to the influence of a magnetic field on *in vitro* drug-release behavior. These matrices were evaluated as possible magnetic responsive delivery systems suitable for controlled release devices.

EXPERIMENTAL

Materials

The PVA (Riedel-de Haën) used presented a saponification value of 87% and an average molecular weight of 22,000. GTA solution (25% w/w) was provided by J. Baker (USA). SCL of molecular weight 4.5×10^5 was provided by CarboMer (USA) and used at 2% w/w in all preparations. Th ($\text{C}_7\text{H}_8\text{N}_4\text{O}_2$, MW = 180.17), in compliance with British Pharmacopoeia standards, was purchased from Saporiti Laboratories (Argentina). This model drug was chosen for drug-release studies because of its stability in water solutions and its easy detection by UV absorption, and it was used in all matrices at 0.2% w/w.

To prepare the ferrofluid, we used $\text{FeCl}_2 \cdot 6\text{H}_2\text{O}$, $\text{FeCl}_3 \cdot 3\text{H}_2\text{O}$, and NH_3 of analytical grade. The surfactant cetyltrimethylammonium bromide (CTAB) was purchased from Sigma (St. Louis, MO).

Methods

Preparation of ferrofluid

The detailed synthesis of magnetite was described earlier.¹² To produce particles with narrow size distribution, magnetite sol was prepared from FeCl_2 and FeCl_3 in an aqueous solution. The ratio between $\text{Fe}^{3+}/\text{Fe}^{2+}$ was two. For the precipitation, we used a solution of NH_3 50% w/w, carefully added with intensive stirring. The magnetite aqueous ferrofluid was synthesized by us in water.¹⁹ To prevent the aggregation between particles and to stabilize the colloid is necessary to generate an additional repulsion force to counterbalance the Van der Waals forces. This can be accomplished by the addition of a surfactant producing a steric stabilization or adding a repulsion agent, such as HClO_4 . In the preparation used in this work, the biocompatible cationic surfactant CTAB was employed. The suspension of magnetite particles with modified surface was treated by sonication for 1 h to obtain a homogeneous system.

Preparation of magnetic hydrogels loaded with theophylline

PVA-based composites. PVA-based composites were prepared by taking an aliquot of the aqueous ferrofluid (0.05 g of particles/milliliters) previously sonicated for 10 min, adding it to PVA solution (6% w/v) and maintaining the mixture under sonication for

30 min. GTA was used at 0.06% w/w as the crosslinking agent to form the gel in the presence of the required amount of Th aqueous solution. The degree of crosslinking (moles of monomer units per mol of crosslinking agent) was 200. A low GTA concentration was used to care for the biocompatibility of PVA gel, affected by residual aldehyde. However, for *in vivo* applications of these PVA composites, further treatment to block any unreacted aldehyde group is advisable, as has been described by Chen et al.²⁴ PVA films were obtained keeping the ferrogels in Petri dishes at low humidity in a sealed container with silica gel for 1 week. A homogeneous particle distribution in PVA films is attained. Nevertheless, after gelification, some agglomeration of particles is produced giving particle aggregates of about 1 μm diameter, as observed by environmental scanning electron microscopy (see below). For some drug-release experiments, the sample was kept under the same uniform magnetic field (600 G with field lines parallel to the surface of the sample) for a number of hours, obtaining a pretreated material.

SCL-based composites. SCL concentration was kept constant in all experiments (2% w/w) by using 0.20 g SCL/10 g of total system (Th, distilled water, ferrofluid, and SCL). The necessary amount of polymer powder was dispersed in water containing the dissolved Th. These dispersions, added with the ferrofluid, were kept stirring at constant temperature for 96 h to obtain the proper polymer swelling and homogeneous gel formation. Well-defined stirring conditions were kept constant for every gel preparation.

Magnetic particles were present at 2.8 and 2.0% w/w in PVA and SCL composites, respectively, determined by weighting the residuum at 600°C.

Environmental scanning electronic microscopy

Compared to traditional scanning electron microscopy (SEM), the most prominent advantage of ESEM is that the imaging of a sample is performed under the protective atmosphere of water vapor. This non-destructive technique allows the imaging of surfaces of practically any specimen wet or dry, insulating or conducting, without any previous treatment of the sample.^{25,26}

Hydrophilic samples such as hydrogels remain intact and the observed topography represents the actual surface structure of the material. ESEM was used as a direct technique to estimate the pore size, as the network mesh or pore size is one of the important parameters in controlling the release rate.

Micrographs of SCL and PVA matrices with or without magnetite particles were obtained at 20°C using a Environmental Scanning Electron Micro-

scope 2010 (FEI Company, Hillsboro, OR) running in the so-called environmental wet mode.

The sample chamber was kept at a constant pressure of 10–20 Torr (1 Torr \cong 133 N m⁻²) displayed at the bottom of each micrograph. The electron beam used had a voltage of 20 kV.

Dynamic rheology

A weighed sample of each gel was used to completely fill up the 1-mm gap space under a 50 mm diameter of a rough flat plate device of a Paar Physica controlled stress rotational shear rheometer (MCR 300, Stuttgart, Germany). The temperature of the sample was kept constant at 25°C using a Peltier system (Viscotherm VT2, Paar Physica, Germany).

Drying out of the samples was prevented by creating a water-saturated atmosphere around them using a small container with distilled water. After the loading of each sample, a 10 min delay was set to reach thermal and mechanical equilibrium to reconfigure the unperturbed state of the samples before any testing.

The linear viscoelastic range (LVR) was determined for each sample performing oscillatory stress sweeps from 0 to 50 Pa at a constant frequency of 2 Hz. The LVR is the range stress/strain within which the measured rheological parameters are constants.

After the LVR was found, a constant strain of 1% was selected to perform the frequency sweep from 0.05 to 4 Hz.

The rheological parameters obtained from the frequency sweeps are the storage modulus (G'), the loss modulus (G''), and the tangent of the phase shift angle ($\tan \delta = G''/G'$). The frequency chosen to compare these parameters was 2 Hz.

Characterization of solids

Adsorption of PVA on the surface of magnetite in films was examined by infrared spectroscopy by a ThermoNicolet FTIR Avatar 320 (Fig. 1).

The magnetization curve of particles dried from a sample of ferrofluid was obtained with a Lakeshore 7300 vibrating sample magnetometer (VSM) at room temperature (Fig. 2).

in vitro drug-release measurements

Assays for *in vitro* Th release from both types of composites were performed in a Flat Ground Joint-type Franz Cell (PermeGear, USA). A Franz cell is a device with two vertical compartments. The upper donor chamber is filled with the gel sample and the lower one is the receptor compartment, initially filled with distilled water. In the lower compartment,

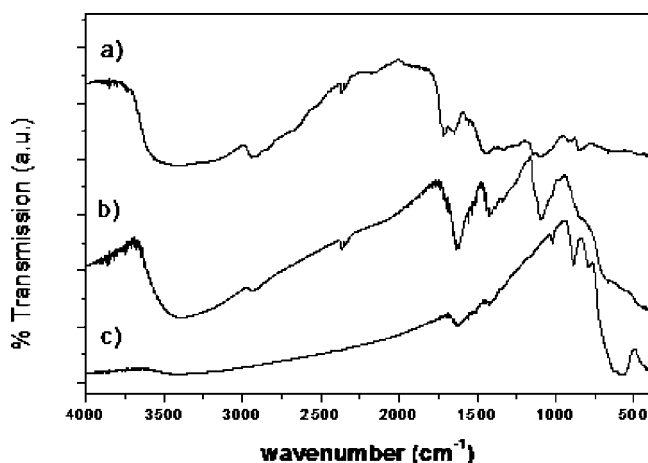


Figure 1 IR spectra of (a) film dried from a PVA 6% w/w aqueous solution, (b) film dried from a sonicated mixture of PVA 6% w/w aqueous solution and magnetite particles, and (c) magnetite particles dried from a ferrofluid sample.

the theophylline concentration increases as drug permeation occurs and samples are taken at different times. The area at the top of the receptor chamber is covered by a membrane sustaining the gel being tested for drug release. In our experiments, a membrane of cellulose (Arthur Thomas, USA) was placed between the upper section of the Franz cell and the lower receptor compartment. The pore size of the hydrophilic cellulose membrane (48 Å) provided a MW cut-off of 12,000. Taking into account the drug size (Th radius: 3.8 Å²⁷), the membrane pores did not introduce an additional restriction. During the release experiments, the composite gel matrix containing the dissolved drug was placed in the upper compartment of the Franz cell. To test the magnetic effect on drug-delivery pattern, a magnetic field of 600 G was applied on the donor compartment of the Franz cell, with magnetic field lines parallel to the release surface of the matrix. The gel sample was placed between the magnetic poles in a region with a mainly uniform field.

The kinetic experiments were performed under thermostatic control (25°C). Because of the magnetic characteristic of the samples, the constant stirring of the receptor compartment was achieved using a mechanical stirrer specially designed for this experimental setup.

Measurements of drug concentration were performed by taking samples of 0.30 mL with a precision syringe at fixed times from the sampling port of the receptor compartment. The Th absorbance was measured at 271 nm in a Shimadzu UV-2401 spectrophotometer (Shimadzu, Kyoto, Japan). After each aliquot was taken, the volume (20 mL) in the receptor compartment was topped-up with distilled water, assuring a constant volume and a full contact

between the polymeric matrix supported by the membrane and the receptor fluid.

Release data treatment

The cumulative concentration of drug released was calculated (determined molar absorption coefficient of Th at 271 nm in water = $1.0 \times 10^4 \text{ M}^{-1} \text{ cm}^{-1}$) and the curves of Th concentration as a function of time were plotted. For each set of experimental conditions, data from replicated experiments were plotted as a group. Therefore, in all cases, the total number of experimental points considered for fitting purposes was in the order of 30–50. Experimental points were normalized using the highest Th concentration delivered when no magnetic field was applied.

Taking into account that the only area available for drug release is the surface of the membrane in contact with the liquid of the receptor compartment of the Franz diffusion cell, an assumption was made that the release process is one dimensional. The data were fitted only at short times (up to 6000–8000 s) to maintain nearly perfect sink conditions, i.e., low drug concentration in the release medium. The temporal behavior of Th concentration during this first part of the release process was adjusted to a power-law type semiempirical equation:^{28,29}

$$M_t/M_\infty = kt^n \quad (1)$$

where, M_t and M_∞ are the cumulative amount of drug released after a time t and an infinite time, respectively, k is a constant depending on kinetic characteristics and experimental conditions, and n is the exponent describing the release process. M_∞ and k were included in k' , and eq. (2) was used to fit the data:

$$[\text{Th}] = k't^n \quad (2)$$

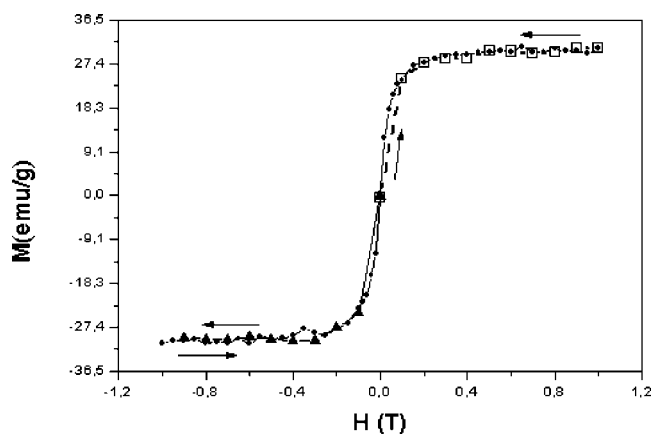


Figure 2 Magnetization versus magnetic field at room temperature for particles dried from a ferrofluid sample. Arrows indicate the sweep of the magnetization curve. □: first step, ●: second step, and ▲: third step of this curve.

where [Th] is the normalized molar concentration of Th in the receptor compartment at time t . The power law [eqs. (1) or (2)] can be seen as an expression that involves two independent mechanisms of drug transport, a Fickian diffusional release because of a chemical potential gradient and a relaxational release because of the swelling in water of hydrophilic polymers (case-II transport). In this last case, the relaxation process of the macromolecules occurring upon water imbibition into the system is the rate-determining stage.

It was used as a global analysis of different replicate experiments using nonlinear least-squares procedure by the Levenberg–Marquardt method (Matlab version 6.5, The MathWorks, 2002). The 95% confidence interval of the nonlinear least square estimation was obtained for all parameters.

RESULTS AND DISCUSSION

Figure 1 shows the infrared spectra of a pure PVA film [Fig. 1(a)], a PVA-magnetite film [Fig. 1(b)], and magnetite particles [Fig. 1(c)]. As shown in Figure 1(a), three absorption bands are observed at 3420, 2930, and 2347 cm^{-1} being assigned to O–H and two C–H stretching of PVA, respectively, while absorption bands assigned to the C–O stretching vibration of PVA are observed at 1620 and 1088 cm^{-1} . In Figure 1(b), these absorption bands are observed at slightly lower wave number. In Figure 1(c), we can appreciate between 1634 and 500 cm^{-1} absorption bands assigned to iron oxides. The intensity of the band of iron oxide near 500 cm^{-1} is not observed in the PVA-magnetite sample. These results indicate that PVA is adsorbed on the surface of the magnetite particles.¹²

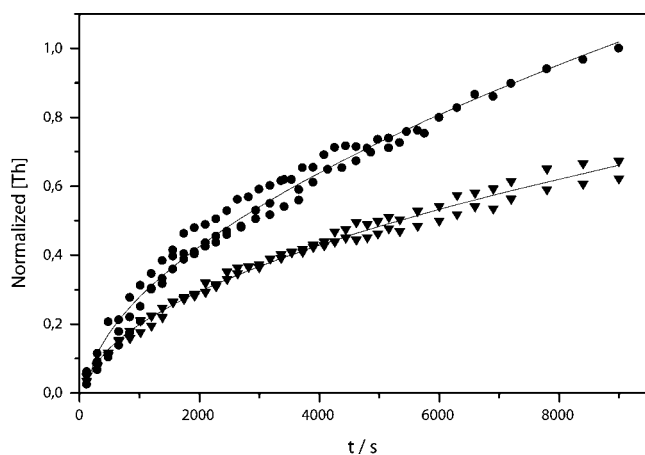


Figure 3 SCL-based composite. Normalized cumulative concentration of Th as a function of release time: (●) without applied magnetic field, (▼) with an applied magnetic field of 600 G. Lines represent calculated values according to eq. (2). Best fit parameters were taken from Table I.

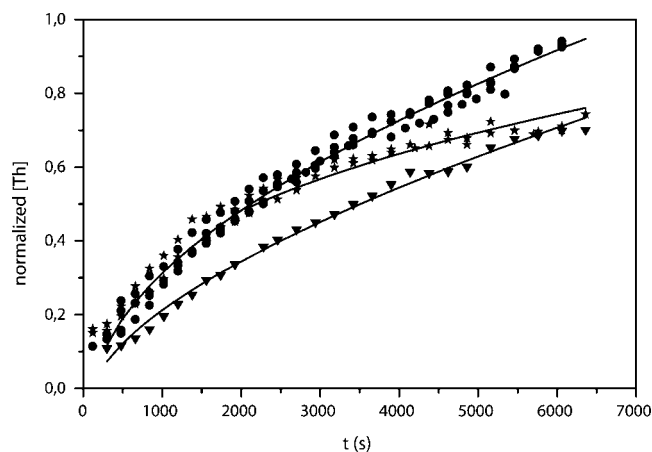


Figure 4 PVA-based composite. Normalized cumulative concentration of Th as a function of release time: (●) without applied magnetic field, (★) with an applied magnetic field of 600 G, (▼) sample maintained 20 h with an applied magnetic field of 600 G and measured under the same magnetic field. Lines represent calculated values according to eq. (2). Best fit parameters were taken from Table II.

Figure 2 shows the magnetization loop of the particles dried from a sample of ferrofluid versus applied field at room temperature. We can appreciate a superparamagnetic behavior, as evidenced by zero coercivity and remanance on the magnetization loop. To describe the magnetization of the magnetic fluid, several theoretical models are used, but the simplest one is Langevin's model and Chantrell method.³⁰ From the corresponding data fitting to the magnetization curve, the magnetic moment μ of each particle is obtained. The particle diameter D is given by the following equation:

$$D = \sqrt[3]{\frac{6\mu}{M_s\pi\rho}} \quad (3)$$

where μ ($2116 \mu_B$)¹⁹ is the magnetic moment of each particle, M_s is the specific saturation magnetization (29.5 emu/g, Fig. 2), and ρ is the density of the iron oxide ($\approx 5.0 \text{ g/cm}^3$). In this case, the particle diameter appears to be in the order of 13.0 nm.¹²

Figures 3 and 4 show the drug-release patterns. The lower curve included in Figure 3 was obtained in the presence of a magnetic field that was applied on the SCL gel matrix at the beginning of the release experiment. Figure 4 incorporates results obtained in two different conditions: applying the magnetic field on the PVA matrix when the release measurements started and using a pretreated material during 20 h.

The nonpretreated PVA gel shows the same release profile with or without magnetic field until 2100 s when both curves start to split. The application of the magnetic field produces a lower release

TABLE I
Theophylline-Release Kinetic Parameters^a Obtained for SCL-Magnetite Hydrogels at Different Conditions (25°C)

External magnetic field	n^b	k^b (s ⁻ⁿ)	R^2
Nonapplied	0.56 ± 0.03	(6.0 ± 1.0) × 10 ⁻³	0.9793
Applied	0.52 ± 0.02	(5.6 ± 1.0) × 10 ⁻³	0.9881

^a Mean and confidence intervals are informed. Statistical treatment of results is mentioned in Experimental section. All parameters are within the 95% confidence interval of the nonlinear least square estimate.

^b Kinetic parameters were obtained by fitting the data through eq. (2).

after a period of time that could be related to a significant particle orientation in the matrix as a consequence of the applied magnetic field. In the case of the pretreated material, the release is lower (compared to the matrix measured in the absence of applied magnetic field) from the beginning of the experiment. Both pretreated and nonpretreated samples attain the same Th concentration at about 6500 s, which could be attributed to the required duration to reach a similar particle alignment in both the nonpretreated sample and the pretreated one.

It has to be noted that in the case of SCL matrix, a less structured system than PVA films, the difference in release kinetics is observed at about 350 s from the starting of the experiment (Fig. 3), pointing to a lower orientation time.

For slab geometry of the sample, the n parameter in eq. (2) has two proposed physical meanings: $n = 0.5$ (diffusion-controlled drug release) and $n = 1.0$ (relaxation-controlled drug release).²⁹ Values of n between 0.5 and 1 can be regarded as a superposition of the two mechanisms mentioned before. Tables I and II present the results of eq. (2) fit for both composites. Data appear to be correctly described and fitted by this equation, as can be seen in Figures 3 and 4 and as it is reflected by the correlation coefficients (R^2) in the range 0.9671–0.9932. The information shown in Tables I and II, where n values are in the range 0.4–0.6, and most cases around 0.5, indicates a predominant diffusion process responsible for drug release. It has to be noted that the case described in the second row of Table II with n near 0.4 and the lowest R^2 is a particular one, because

during the first part of the release, a well structured network like a PVA film, is affected by modifications in particle alignment, probably leading to a distorted release pattern.

We can appreciate that the application of a magnetic field parallel to the release surface of the gel decreases the amount of drug delivered, in both matrices. This behavior is in agreement with the recent results reported by Liu et al.,¹⁴ who found a change from rapid to slow drug release by the application of an external magnetic field. This behavior is attributed to a considerable reduction of the pore size and an increased tortuosity of the pore channels of the composite hydrogel, both facts leading to a decreased drug release.

Under a uniform magnetic field, the applied field orients magnetic dipoles and particle–particle interactions become important.³¹ The particles attract each other when aligned end-to-end, as has been shown for Fe₃O₄ particles dispersed in silicon oil under a uniform magnetic field.¹¹ The smaller drug release reported in this work for both composites under the influence of applied magnetic field can be explained taking into account that the orientation of magnetic dipoles of particles dispersed in the polymeric matrix causes the formation of row structures, parallel to the field direction. As a result, these chainlike structures may restrict the diffusion of Th by increasing the tortuosity of pore channels filled with the aqueous phase.

Moreover, a temporary reinforcement effect has been described for a uniform magnetic field applied on a magnetic gel. This effect leads to an increase in

TABLE II
Theophylline-Release Kinetic Parameters^a Obtained for PVA-Magnetite Hydrogels at Different Conditions (25°C)

External magnetic field	n^b	k^b (s ⁻ⁿ)	R^2
Nonapplied	0.55 ± 0.03	(7.3 ± 1.8) × 10 ⁻³	0.9865
Applied on nonpretreated sample	0.37 ± 0.03	(3.1 ± 0.8) × 10 ⁻²	0.9671
Applied on pretreated sample	0.62 ± 0.05	(3.1 ± 1.4) × 10 ⁻³	0.9932

^a Mean and confidence intervals are informed. Statistical treatment of results is mentioned in Experimental section. All parameters are within the 95% confidence interval of the nonlinear least square estimate.

^b Kinetic parameters were obtained by fitting the data through eq. (2).

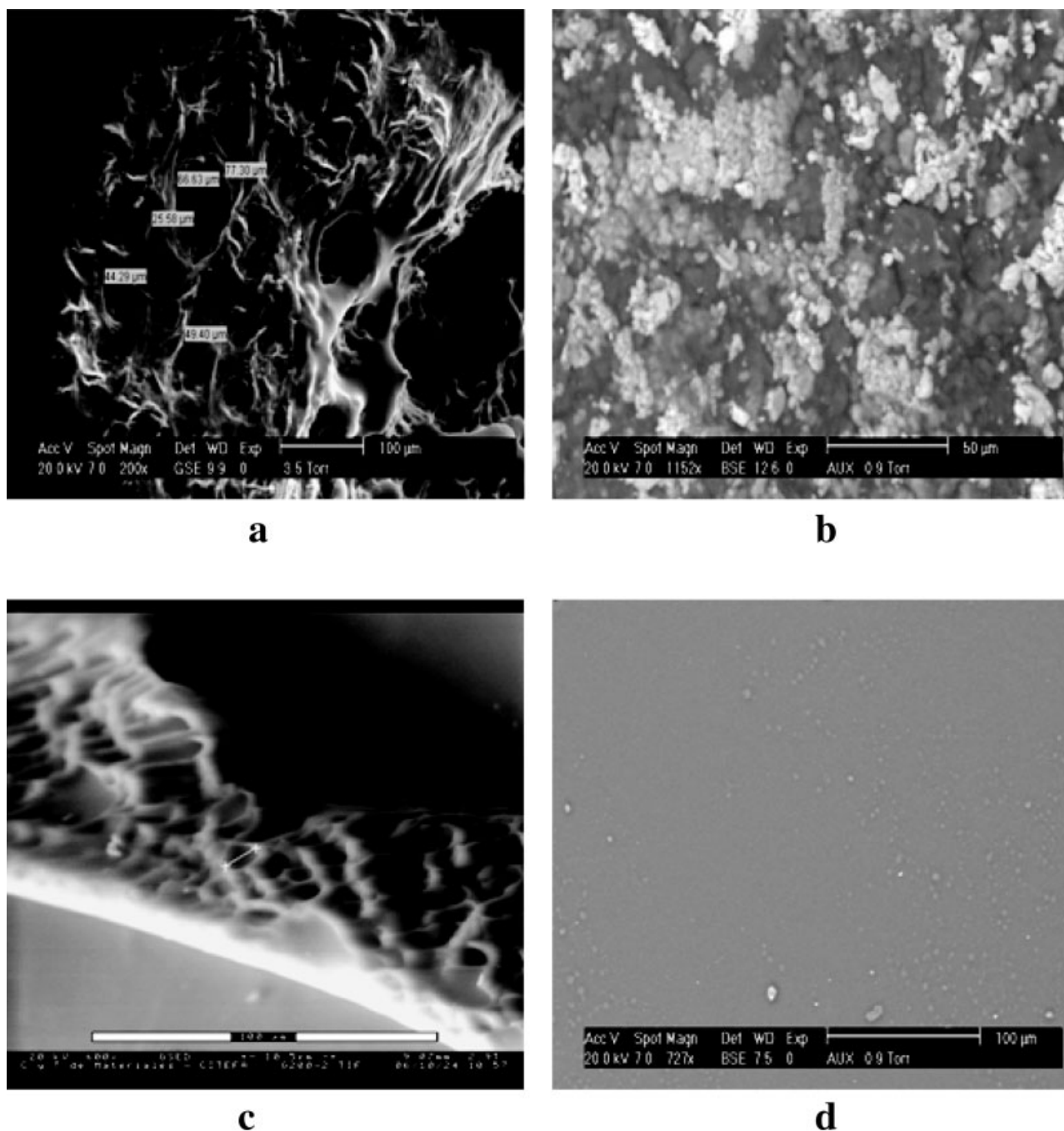


Figure 5 ESEM micrographs of (a) SCL 2% w/w without particles (b) SCL 2% w/w with 2.0% w/w particles; (c) PVA film without particles, and (d) PVA film with 2.8% w/w of magnetite particles.

the elastic modulus (G') of the material, meaning that the deformation of the ferrogels requires more energy under a uniform magnetic field.¹¹ The G' parameter can be used as an indicator of macroscopic hardness and as an indicator of structure.³² These considerations are related to the increase of viscosity observed in ferrofluids under a magnetic field.³³ Results obtained in our laboratory showed that in an aqueous ferrofluid with 1.8% w/w particle concentration, the viscosity (0.946 cp at room tem-

perature and in the absence of a magnetic field) increases up to 30% when a magnetic field of 600 G is applied.

For SCL gels (with no added magnetic particles), in our previous work,²² an increased elastic modulus with growing polymer concentration has been observed, concurrently with a lower drug release. In that work, the elastic modulus G' , which is proposed to be directly related to the crosslink density of the network,³⁴ showed an increase when the SCL

concentration changed from 1% w/w ($G' = 49$ Pa) to 4% w/w ($G' = 445$ Pa). This more solid matrix was coupled with the observation of a 20% decrease in drug release at 3500 s.

From the frequency sweeps of rheological experiments, it can be concluded that the matrices studied herein are weak gels because G' and G'' exhibit a light frequency dependence with no sign of a Newtonian plateau in the low-frequency region, being G' always bigger than G'' thus resulting in a solidlike behavior.³⁵

The application of magnetic field to the composites studied in this work may also increase the hardness of gel system and this fact can account for the observed lesser drug release. To better understand the effect of magnetic particles inclusion, we measured G' for a composite made of 1% w/w magnetite particles and 2% w/w SCL gel and we compared the G' value with that obtained for a 2% w/w SCL gel without particles.²³ The experimental results point to a bigger rigidity of the systems after the inclusion of the magnetic particles. The matrix loaded with particles shows a wider LVR (0–23 Pa) than that of the material without particles (0–15 Pa) and also presents a reinforcement of the elastic modulus (from 117 ± 8 Pa to 178 ± 17 Pa). This effect is probably due to the magnetic interactions between particles. The same effect is observed for other systems using polyvinyl alcohol as hydrogel.³⁶

To test the influence of the magnetic field on G' , we placed the SCL-magnetite material under an external uniform field of 600 Gauss during 20 or 69 h before the rheological test. A 20-h pretreated material showed a 30% increase in the G' modulus when compared with the value obtained for the nonpretreated one. Furthermore, it was observed an increase of 95% in G' when comparing a 20-h pretreated system with a 69-h pretreated one, indicative of a bigger rigidity of the matrix as the pretreatment time increases.

In an attempt to identify the composite morphology, ESEM micrographs were obtained for both systems. Experimental conditions are detailed at the bottom of each one (Fig. 5). Figure 5(a,b) are micrographs for a 2% w/w SCL matrix without and with magnetic particles, respectively. Figure 5(c,d) correspond to PVA matrix without or with magnetite particles in that order.

Figure 5(a) shows a spongelike gel structure with pore sizes ranging from 40 to 77 μm . Figure 5(b) illustrates a very different situation, where the particles tend to add to form larger aggregates and the opened structure observed in Figure 5(a) is not preserved.

Figure 5(c) shows a micrograph of a PVA film on the edge pores with a size of about 11 μm can be seen.

From Figure 5(d), it can be observed that magnetic particles, forming agglomerates mostly around 2–3 μm , are well distributed in a compacted PVA matrix.

For both matrices, a considerable more open structure is observed without particles in comparison with that obtained with the inclusion of particles. The pore diameter drops drastically when particles are present, possibly leading to an increase in the tortuosity of inner channels filled with the aqueous phase. In the presence of a magnetic field, the formation of particle row structures results in a decreased drug release.

Additional research will allow us to evaluate drug-release behavior under the influence of a number of factors such as particle concentration, direction of the applied magnetic field relative to the drug release flow path, and intensity of the magnetic field.

CONCLUSIONS

Two biocompatible composite gels containing magnetic particles and loaded with theophylline have been prepared and tested as drug-delivery matrices. The experimental data show that the drug-release kinetics can be decreased by the application of a uniform magnetic field. These results can be explained by the effects of the added particles to the gel, which leads to an increase of the rigidity of the matrix and a less opened structure. For some purposes, a reduced drug delivery could be an advantage, depending on expected drug effect. For example, a slower release will bring a wider delivery time.

These results suggest that these composites offer promising capabilities for their application in controlled drug-delivery systems responsive to external stimuli, such as an external magnetic field.

The authors are grateful to Mrs. Paula Bertoglio for her assistance in particle preparations. The authors thank Dr. Marta Rosen (Head of Group of Porous Media, Facultad de Ingeniería, Universidad de Buenos Aires) for the use of the dynamic rheometer.

References

1. Moghimi, S. M.; Hunter, A. C. H.; Murray, J. C. *Pharm Rev* 2001, 53, 283.
2. Gupta, A. K.; Gupta, M. *Biomaterials* 2005, 26, 3995.
3. Gilchrist, R. K.; Medal, R.; Shorey, W. D.; Hanselman, R. C.; Parrot, J. C.; Taylor, C. B. *Ann Surg* 1957, 146, 596.
4. Schwertmann, U.; Cornell, R. M. In *Iron Oxides in the Laboratory: Preparation and Characterization*; VCH: Weinheim, 1991; Chapter 1.
5. Neuberger, T.; Schöpf, B.; Hofmann, H.; Hofmann, M.; Von Rechenberg, R. *J Magn Magn Mater* 2005, 293, 483.
6. Yang, J.; Lee, H.; Hyung, W.; Park, S.-B.; Haam, S. *J Microencapsul* 2006, 23, 203.

7. Qiu, Y.; Park, K. *Adv Drug Deliv Rev* 2001, 53, 321.
8. Zrínyi, M.; Barsi, L.; Büki, A. *J Chem Phys* 1996, 104, 8750.
9. Ramanujan, R. V.; Lao, L. *Smart Mater Struct* 2006, 15, 952.
10. Chatterjee, J.; Haik, Y.; Chen, C. *J Colloid Polym Sci* 2003, 281, 892.
11. Varga, Z.; Filipcsei, G.; Szilágyi, A.; Zrínyi, M. *Macromol Symp* 2005, 227, 123.
12. Albornoz, C.; Sileo, E. E.; Jacobo, S. E. *Phys B: Condens Matter* 2004, 354, 149.
13. Zrínyi, M.; Barsi, L.; Buki, A. *Polym Gels Netw* 1997, 5, 415.
14. Liu, T. Y.; Hu, S. H.; Liu, T. Y.; Liu, D. M.; Chen, S. Y. *Langmuir* 2006, 22, 5974.
15. Scotchford, C. A.; Cascone, M. G.; Downes, S.; Giusti, P. *Biomaterials* 1998, 19, 1.
16. Jayakrishnan, A.; Jameela, S. R. *Biomaterials* 1996, 17, 471.
17. Chen, P.-R.; Kang, P.-L.; Su, W.-Y.; Lin, F.-H.; Chena, M.-H. *Biomed Eng Appl Basis Comm* 2005, 17, 44.
18. Chatterjee, J.; Haik, Y.; Chen, C. *J BioMagn Res Technol* 2004, 2, 2. Available at www.biomagres.com/content/2/1/2
19. Albornoz, C.; Jacobo, S. *J Magn Magn Mater* 2006, 305, 12.
20. de Nooy, A. E. J.; Rori, V.; Masci, G.; Dentini, M.; Crescenzi, V. *Carbohydr Res* 2000, 324, 116; and references therein.
21. Daraio, M. E.; François, N. J.; Bernik, D. L. *Drug Deliv* 2003, 10, 79.
22. François, N. J.; Rojas, A. M.; Daraio, M. E.; Bernik, D. L. *J Controlled Release* 2003, 90, 355.
23. François, N. J.; Rojas, A. M.; Daraio, M. E. *Polym Int* 2005, 54, 1613.
24. Chen, P.-R.; Chen, M.-H.; Lin, F.-H.; Su, W.-Y. *Biomaterials* 2005, 26, 6579.
25. Micic, M.; Radotic, K.; Benitez, I.; Ruano, M.; Jeremic, M.; Moy, V.; Mabrouki, M.; Leblanc, R. *Biophys Chem* 2001, 94, 257.
26. Schalek, R.; Drzal, L. *J Adv Mater* 2000, 32, 32.
27. Amsden, B. *Macromolecules* 1998, 31, 8382.
28. Ritger, P. L.; Peppas, N. A. *J Controlled Release* 1987, 5, 23.
29. Ritger, P. L.; Peppas, N. A. *J Controlled Release* 1987, 5, 37.
30. Chantrell, R. W.; Popplewell, J.; Charles, S. W. *IEEE Trans Mag* 1978, 14, 975.
31. Szabó, D.; Czakó-Nagy, I.; Zrínyi, M.; Vértes, A. *J Colloid Interface Sci* 2000, 221, 166.
32. Narine, S.; Marangoni, A. *Lebensm-Wiss u-Technol* 2001, 34, 33.
33. McTague, J. P. *J Chem Phys* 1969, 51, 133.
34. Axelos, M. A. V.; Lefebvre, J.; Qiu, C. G.; Rao, M. A. In *The Chemistry and Technology of Pectin*; Walter, R. H., Ed.; Academic Press: San Diego, CA, 1991; Chapter 11.
35. Lapasin, R.; Pricl, S. *Rheology of Industrial Polysaccharides, Theory and Applications*. Blackie: Glasgow, 1995; Chapter 4.
36. Hernández, R.; Sarafian, A.; López, D.; Mijangos, C. *Polymer* 2004, 46, 5543.